REGRIDDING OF REMOTE SOUNDING MEASUREMENTS AND APPLICATION TO OZONE PROFILE INTERCOMPARISONS

Yasmine Calisesi[(1)] and Vincent T. Soebijanta[(2)]

[(1)]International Space Science Institute, Bern, Switzerland
Hallerstrasse 6, CH–3012 Bern, Switzerland
yasmine.calisesi@issi.unibe.ch
[(2)]Belgian Institute for Space Aeronomy, Uccle, Belgium
† November 14, 2003

ABSTRACT

One of the difficulties arising when intercomparing remote sensing observations of atmospheric constituents profiles consists in homogenizing their respective vertical coordinates to allow quantitative results comparison. Simple profile interpolation is often unsatisfactory in this case, as the retrieval vertical grid constitutes an integral part of the retrieved vector which should be accounted for in subsequent profile transformations. Recently, a method of comparing remote sounders while allowing for different observational characteristics was proposed by *Rodgers and Connor* [1]. Unfortunately, application of this method was first restricted to the comparison of identical state vectors. We propose to relax this condition, by the use of a linear transformation function to homogenize the units and vertical grids of different retrievals results.

1. INTRODUCTION

Two main difficulties are associated with the intercomparison of atmospheric remote soundings. The first difficulty arises from the basic nature of remote sensing measurements. Solutions to the underlying ill-posed problems are indeed not uniquely determined by the state of the atmosphere, but result rather from a trade-off between information extracted from an observed signal, which depends in a known way on the searched quantity, and some additional, regularizing information used to constrain the inverse problem towards physically acceptable solutions. The share of information actually contributed by the measurements to the retrieval results, or the influence of other determining factors such as forward model parameters, spectral resolution, or measurement errors, is generally not uniform over the considered retrieval range and depends on the observing system configuration. In intercomparison procedures, these characteristics must be taken into account in order to ensure a correct interpretation of the intercomparison results.

This problem was recently addressed by *Rodgers and Connor* [1], who proposed to account for differing observing systems characteristics by identifying and gradually eliminating the corresponding bias contributions from the obtained comparison results. These contributions are commonly assimilated to the retrieval smoothing error [2, 3, 4], and arise from 1) the use of different a-priori information with different observing systems, 2) the use of different estimation rules in the inverse model, 3) the achievement of different vertical resolutions and sensible altitude ranges, and 4) the measurement of different sub-spaces of the state space by each observing system. Correction for these differing characteristics is achieved by "normalizing" each retrieved profile to generic values applying to the overall comparison ensemble. This approach constitutes an essential step in the interpretation of remote sounders intercomparisons results. Unfortunately, it was originally restricted to comparisons of identical state vectors.

This restriction relates to the second difficulty generally encountered when intercomparing remote sensing measurements, namely, the inhomogeneity of the comparison data. As a matter of fact, two independent profile measurements to be compared to each other will generally be expressed in different units, and will be characterized by fully different vertical and temporal resolutions. In the case of atmospheric remote sounders, the difficulty is even increased by the discretization of the sought continuous atmospheric constituents profile onto a given numerical computation grid. This procedure goes along with the assumption of discretization rules, which are inextricably bound to the achieved retrieval results. The problem of homogenizing the retrieval coordinates for comparison purposes is seemingly trivial, but is still worth consideration as systematic uncertainties added to a retrieved profile by its simple interpolation to a different vertical grid might significantly affect its comparison results. In addition, the use of different vertical retrieval grids by different remote sensing systems hampers the detailed evaluation of comparison results according to the above method, as the latter implies the manipulation of other dependent retrieval products as averaging kernels and covariance matrixes. The purpose of the present study is to extend the application of [1], by the

Proc. of the 2004 Envisat & ERS Symposium, Salzburg, Austria
6-10 September 2004 (ESA SP-572, April 2005)

use of a linear transformation to homogenize different representations of a single target profile and associated retrieval matrixes.

2. HOMOGENIZATION OF THE RETRIEVAL PRODUCTS

2.1 Products Regridding

Following the nomenclature of [5], we note $\mathbf{x}$ the $m \times 1$ vector of the atmospheric state to be retrieved ("state vector"), and $\mathbf{y}$ the $n \times 1$ vector of the measured signal ("measurement vector"). $\mathbf{x}$ may contain, besides atmospheric constituents concentration profiles or other aerological parameters, also a number of instrumental variables which we suppose to be left unchanged by the discussed numerical grid transformation. The measurement vector $\mathbf{y}$ is related to the state vector $\mathbf{x}$ by the forward model

$$\mathbf{y} = \mathbf{F}(\mathbf{x}) + \boldsymbol{\epsilon} \tag{1}$$

where $\mathbf{F}(\mathbf{x})$ describes the physics of the measurement, and should include every known process influencing the measured signal until its detection in the instrument. It reproduces the actual measurement within accuracy $\boldsymbol{\epsilon}$, which encapsulates any systematic and random components of the forward model and measurement errors.

In the case of linear or weakly non-linear problems, the forward model (1) can be developed into a Taylor expansion about some arbitrary reference point $\mathbf{x_0}$ [6]:

$$\mathbf{y} = \mathbf{F}(\mathbf{x_0}) + \mathbf{K_x}(\mathbf{x} - \mathbf{x_0}) + \boldsymbol{\epsilon} \tag{2}$$

where $\mathbf{K_x} = (\partial \mathbf{F}/\partial \mathbf{x})_{\mathbf{x_0}}$ is the $n \times m$ matrix of the weighting functions. Regularization of this inverse problem with the help of a-priori information leads to the solution [2]

$$\hat{\mathbf{x}} = \mathbf{x_a} + \mathbf{G_x}[\mathbf{y} - \mathbf{F}(\mathbf{x_0}) - \mathbf{K_x}(\mathbf{x_a} - \mathbf{x_0})] \tag{3}$$

or

$$\hat{\mathbf{x}} = \mathbf{x_a} + \mathbf{A_x}(\mathbf{x} - \mathbf{x_a}) + \mathbf{G_x}\boldsymbol{\epsilon} \tag{4}$$

where $\hat{\mathbf{x}}$ is the retrieved quantity, $\mathbf{x}$ is the searched atmospheric constituents or temperature profile, $\mathbf{x_a}$ is the used a-priori profile, $\mathbf{A_x} = \mathbf{G_x}\mathbf{K_x}$ is the $m \times m$ matrix of the averaging kernels, $\mathbf{G_x}$ is the $m \times n$ contribution functions matrix, and $\mathbf{G_x}\boldsymbol{\epsilon}$ is the image, in the profile space, of the measurements and forward model errors.

Suppose now that two independent retrieval procedures are used to infer the atmospheric profile from the measurements $\mathbf{y}$. Ideally, the state vector would be represented in both cases by a continuous function, so that differences between the procedures would be induced only by differences in their respective forward models. In the practice, however, a discrete representation of the state vector is used, introducing differences in the chosen numerical grids as an additional potential source of discrepancy between the respective retrieval results. In the above formalism, we suppose that the numerical grid of $\mathbf{x}$ is fine enough to allow an accurate forward model representation of the measurements $\mathbf{y}$. In order to evaluate the impact of different numerical grid resolutions on the retrieval results, we suppose that a second, slightly coarser representation of the state vector is used. We name $\mathbf{z}$ this new $l \times 1$ state vector representation, with $l < m$. Neglecting in a first time the units transformation problem, we can define an $m \times l$ linear interpolation matrix, $\mathbf{W}$, or an $l \times m$ averaging operator, $\mathbf{W}^*$, such as

$$\mathbf{x} = \mathbf{W}\mathbf{z} + \boldsymbol{\epsilon_W} \tag{5}$$

or

$$\mathbf{z} = \mathbf{W}^*\mathbf{x} \tag{6}$$

where $\mathbf{W}^*$ is a generalized pseudo-inverse of $\mathbf{W}$ [7, 8, 5], and $\boldsymbol{\epsilon_W} = (\mathbf{I} - \mathbf{W}\mathbf{W}^*)\mathbf{x}$ is the error induced by the interpolation rule on the reconstructed high resolution profile.

Combined with (1) to (4), the transformations (5) and (6) allow to derive the transformation rules for the retrieval results, and associated retrieval matrixes, from the fine to the coarse numerical grid. Accordingly, we obtain for the transformation of $\mathbf{K_x}$, $\hat{\mathbf{x}}$, $\mathbf{G_x}$, and $\mathbf{A_x}$:

$$\mathbf{K_z} = \mathbf{K_x}\mathbf{W} \tag{7}$$

and

$$\begin{aligned} &\hat{\mathbf{z}} - \mathbf{z_a} \\ &\quad = \mathbf{W}^*(\hat{\mathbf{x}} - \mathbf{x_a}) - \mathbf{W}^*\mathbf{A_x}(\mathbf{I} - \mathbf{W}\mathbf{W}^*)(\mathbf{x} - \mathbf{x_a}) \end{aligned} \tag{8}$$

when

$$\mathbf{G_z} = \mathbf{W}^*\mathbf{G_x} \tag{9}$$

and

$$\mathbf{A_z} = \mathbf{W}^*\mathbf{A_x}\mathbf{W} \tag{10}$$

Equations (7), (9), (9), and (10) are exact relationships, which allow to transform the retrieved profile $\hat{\mathbf{x}}$ and the associated matrixes $\mathbf{K_x}$, $\mathbf{G_x}$, and $\mathbf{A_x}$ from a fine to coarse retrieval grid, given the transformation rules (5) and (6). Note, however, that the restricted properties of the pseudo-inverse do not allow reciprocity in these equations, so that it will in general not be possible to reconstruct a high resolution product from the low resolution result without the introduction of representation errors.

2.2 Units Transformation

The above formalism expands to the general case by rewriting $\mathbf{W} = \mathbf{Z}\mathbf{U}$, where $\mathbf{Z}$ is a regridding function as in (5) and $\mathbf{U}$ is a square, diagonal units transformation matrix. Equation (5) then transforms to:

$$\mathbf{x} = \mathbf{W}\mathbf{z} + \boldsymbol{\epsilon_W} \tag{11}$$

which is of the same form as (5), but where the error $\epsilon_{\mathbf{W}}$ also encapsulates the image of the units conversion error. Similarly, we obtain for (6):

$$\mathbf{z} = \mathbf{W}^{*}\mathbf{x} + \epsilon_{\mathbf{W}^{*}} \tag{12}$$

where $\epsilon_{\mathbf{W}^{*}}$ is now different from zero and includes the image of the units conversion error. It can easily be shown that the replacement of (5) and (6) by (11) and (12) does not alter the results obtained in Section 2.1 for the transformation of the retrieval products.

3. APPLICATION: INTERCOMPARISON OF OZONE PROFILE OBSERVATIONS

We used the above formalism combined to the method proposed by *Rodgers and Connor* [1] to compare independent ozone profile observations performed during 2000 with the satellite-borne Global Ozone Monitoring Experiment (GOME) [9] and the ground-based millimeter-wave Stratospheric Ozone Monitoring Radiometer (SOMORA) [10].

3.1 Instruments Characteristics

SOMORA provides quasi-continuous observations of the stratospheric and mesospheric ozone volume mixing ratio (VMR) profile. The instrument monitors the rotational transition line of ozone at 142.175 GHz. Information about the species vertical distribution is extracted from the recorded pressure-broadened emission spectra using an iterative optimal estimation retrieval algorithm [6]. The retrieved state vector consists of 29 ozone profile components, complemented with 4 auxiliary observational parameters. The ozone VMR values are retrieved within fixed altitude layers of 2-20 km width distributed between the ground and 110 km altitude. A-priori information is taken from an independent 5-year microwave ozone profile climatology. After 30 minutes integration time, sufficient signal-to-noise is achieved in the SOMORA spectral line measurements to retrieve ozone profiles with low a-priori information content between 20 and 65 km altitude. The corresponding vertical resolution, taken as the width at half-maximum of the observing system averaging kernels, is of the order of 10 km in this altitude range [11]. The SOMORA averaging kernels are represented in Figure 1. The SOMORA instrument was first operated at the Institute of Applied Physics of the University of Bern (46.95°N 7.45°E) in August 1999. In June 2002, the system was moved to Payerne (46.82°N 6.95°E) where it is now operated by the Swiss Federal Institute of Meteorology and Climatology (MeteoSwiss). SOMORA is currently undergoing the process of validation.

GOME was launched on board the second European Remote Sensing satellite (ERS-2) onto a sun-synchronous, near polar orbit on April 21, 1995. It provides measurements of the integrated ozone column within partially

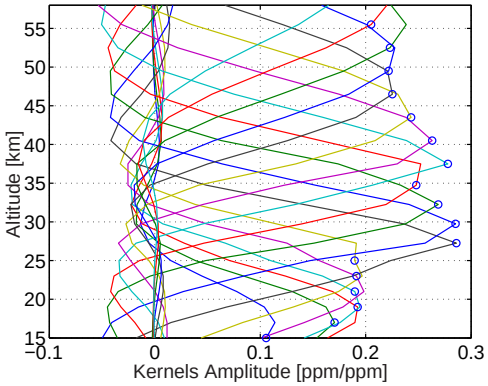

Figure 1: Averaging kernels for the SOMORA ozone VMR retrievals. The nominal height of each kernel is marked by a circle.

variable pressure layers. The instrument measures the solar irradiance and backscattered earthshine radiance in the 240–790 nm spectral band in a nadir viewing geometry. Information about the vertical distribution of ozone in the stratosphere is retrieved from the 265–330 nm ozone absorption band. The GOME level-2 ozone data used in the present study were processed at the Royal Netherlands Meteorological Institute (KNMI) using the Ozone ProfilE Retrieval Algorithm (OPERA). As for the SOMORA retrieval, this algorithm is based on an iterative optimal estimation scheme [6]. The GOME retrieval procedure uses 40 retrieval layers of equal width in log(Pressure). The lowest level is adjusted to the actual surface pressure, and the level closest to the cloud top level is forced to the corresponding pressure value. A-priori information is provided by an hybrid ozone sonde and satellite measurements climatology [12]. With an integration time of 12 seconds, corresponding to a nadir spatial resolution of approximately 100x960 square kilometers, sufficient information is contained in the GOME measurements to retrieve ozone partial column profiles with low a-priori information content from the lower stratosphere up to $\sim$50 km altitude. The vertical resolution of the GOME retrieval results lies between 4 and 8 km depending on altitude. The GOME averaging kernels are represented in Figure 2.

3.2 Data Selection

The accepted coincidence and collocation criterion between the SOMORA and GOME ozone profile measurements was set to maximum $\pm$ 15 minutes integration window and $\pm$ 400 km ground pixel center offset, respectively. This selection criterion yielded a set of 84 coincident and collocated SOMORA and GOME measurements during 2000.

3.3 Profile Homogenization

In order to allow a quantitative comparison of the respective retrieval results, a transformation of the GOME

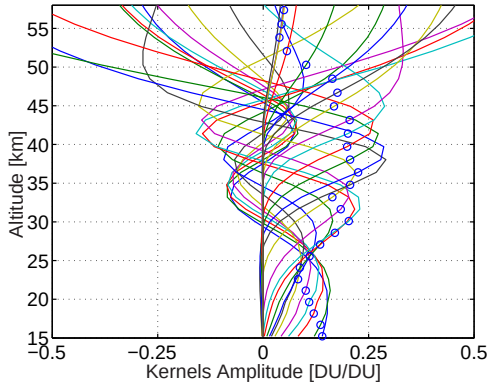

Figure 2: Averaging kernels for the GOME column ozone retrievals. In contrast to Figure 1, these kernels do not peak at their nominal altitude due to the used absolute ozone concentration units.

ozone profiles to the SOMORA coordinates, or conversely, is required. The transformation will be performed according to (11) and (12). While the coefficients of the units conversion matrix $\mathbf{U}$ are easily derived from the appropriate units conversion rule, things are a bit more complicate for the vertical regridding matrix $\mathbf{Z}$ as its definition necessitates the assumption of an interpolation or averaging rule for the one or the other retrieval result. Clearly, this choice should rely on the vertical sampling rules explicitely or implicitly employed in each retrieval procedure for the sought concentration profile.

In the present example, both instruments provide layer averages of the ozone abundance within diversely defined retrieval layers. The GOME retrieval grid is finer than the SOMORA grid, so that the most intuitive choice here consists in defining an averaging function $\mathbf{Z}^*$ to convert the GOME profiles to the coarser SOMORA retrieval grid.

The GOME profiles are column ozone values within variable pressure layers, while the SOMORA results are ozone VMR values within fixed altitude layers. In both cases, the averaging rules assumed in each retrieval procedure conserve column ozone within the retrieval layers. We thus constructed $\mathbf{Z}^*$ by simply rearranging the retrieved GOME column ozone amounts over the overlapping SOMORA layers, proportionally to the respective layers overlap rate. According to this, if g is the number of GOME retrieval layers, and s is the number of SOMORA retrieval layers ($s < g$), then the elements of the $s \times g$ GOME to SOMORA grid transformation matrix are given by:

$$Z_{i,j} = (S_i \cap G_j)/G_j \qquad [\mathrm{m/m}] \qquad (13)$$

where $i = 1..s$, $j = 1..g$, and S_i and G_j denote the vertical range of the i-th SOMORA, respectively j-th GOME retrieval layer.

3.4 Comparison Procedure

In a first step, the GOME profiles were converted to the SOMORA coordinates using the above defined transformation matrix.Due to the day-to-day variability of the GOME retrieval grid, $\mathbf{W}^*$ was defined anew for each comparison day. The respective retrieval results were then intercompared along the SOMORA retrieval grid. In addition, the influence of smoothing error was investigated by applying the method proposed by [1]. For that purpose, the respective retrieval results were successively corrected for the use of different a-priori information, reduced for non-iterative linear retrieval, and the high-resolution GOME profiles were convoluted with the lower-resolution SOMORA averaging kernels. In a second step, a verification of the achieved comparison results was obtained by considering a second series of the SOMORA retrievals, computed firsthand on the GOME retrieval grid. In this case, no adjustment of the respective vertical coordinates was required, allowing direct intercomparison of the GOME and SOMORA retrieval results. The results of these different intercomparison series are presented in Sections 4.1 and 4.2. In all cases, the comparison ensemble a-priori was taken as the SOMORA a-priori. When required, the GOME averaging kernels were transposed to the SOMORA profile coordinates using (10). An example of the transformation of the GOME averaging kernels to the SOMORA retrieval coordinates is represented in Figure 3.

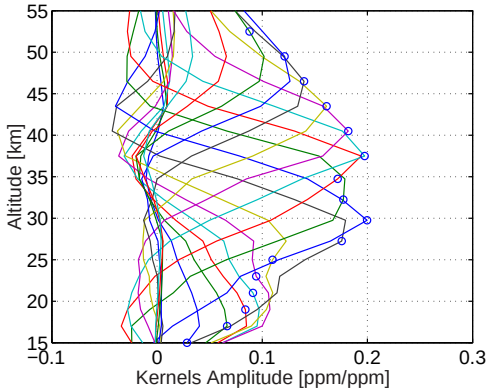

Figure 3: The GOME averaging kernels as seen through the SOMORA instrument. The GOME averaging kernels were transposed to the SOMORA retrieval coordinates, adjusted for the comparison ensemble a-priori, and convoluted with the SOMORA averaging kernels.

4. RESULTS

4.1 GOME Grid Transformation

Figure 4 shows the results of the comparison between coincident SOMORA and GOME ozone profiles along the SOMORA retrieval grid. In the present case, a statistical

analysis of the 1-year comparison ensemble was allowed by the time invariance of the achieved common vertical profile coordinate. The width of the obtained bias distribution ($\pm 2\sigma$, thin solid curves) could then be compared to the expected bias variance ($\pm 2\sigma$, dashed), estimated from the respective retrieval error covariances. For comparison with the following Section, the results for the individual measurement pairs are also represented in a bundle (light grey). Besides a $<5\%$ ($<7\%$) systematic ozone

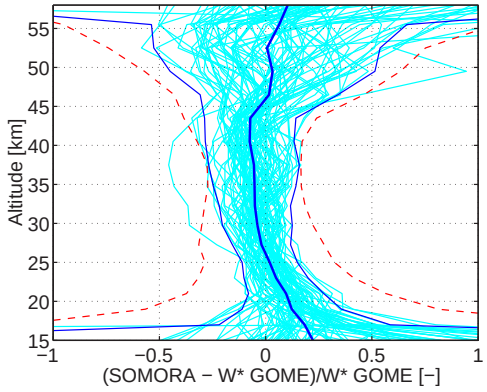

Figure 4: Light grey: relative difference between coincident SOMORA and GOME ozone profiles, GOME profiles transformed to SOMORA retrieval coordinates using (12). Black solid curves: sample average and $\pm 2\sigma$ width. Black dashed curves: expected bias variance ($\pm 2\sigma$) for optimal estimation retrieval results.

underestimation by SOMORA with respect to GOME between 25 and 35 (45) km, the figure reveals an increasing discrepancy between the two observing systems outside of this altitude range. This discrepancy could be induced by differences in the sensible altitude range of the two instruments, i.e. lower than 50 km for the GOME observations and higher than 20 km for the SOMORA measurements, and to the gradual switch towards a-priori information outside of this altitude range. The larger measurements discrepancy above 45 km and below 25 km is also associated to an extreme results variability, with the corresponding 2σ-values reaching 40% at 17 km and 60% at 55 km. Nevertheless, these values still lie within the range of the expected comparison results variance, indicating that potential exists for improving the significance of the comparison results.

Figure 5 shows the results of the comparison after applying the *Rodgers and Connor* [1] procedure. As expected, an improved overall agreement between the SOMORA and GOME measurements is observed at all altitudes with respect to Figure 4. The achieved average bias lies within $\pm 7\%$ at all altitudes, with a maximum underestimation of the SOMORA ozone values with respect to GOME at 35 km. The ensemble standard deviation (2σ) is reduced to 10% at 17 km, 8% at 25

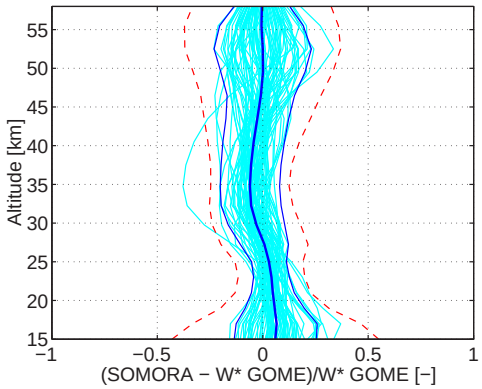

Figure 5: As Figure 4, with SOMORA and GOME results corrected for different a-priori information, optimized with respect to the comparison ensemble a-priori, and GOME profiles convoluted with SOMORA averaging kernels.

km, and 20% at 55 km. These values are consistent with the reduced distribution variance estimated for the comparison results after removal of all smoothing error contributions according to [1].

4.2 Method Verification

A verification of the above results is obtained by considering a second series of the SOMORA retrievals, computed firsthand on the GOME numerical grid. The results of the comparison of this second SOMORA dataset with the coincident GOME observations are shown in Figure 6. This figure reproduces very closely the results obtained in Figure 4, indicating that no significant artefacts were added to the comparison results by the transformation proposed in Section 2.1.

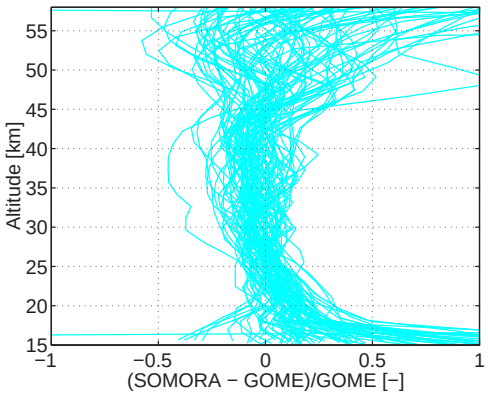

Figure 6: Relative difference between GOME ozone profiles and coincident SOMORA retrievals computed directly on the GOME retrieval grid.

Also, good agreement is achieved in the further comparison steps between the results obtained using the

reprocessed (Figure 7) and original (Figure 5) SOMORA data sets. Apart from a somewhat larger appearant results distribution width, the close similarity of the features obtained in Figure 7 compared to those in Figure 5 tends to confirm the reliability of the proposed profile regridding method.

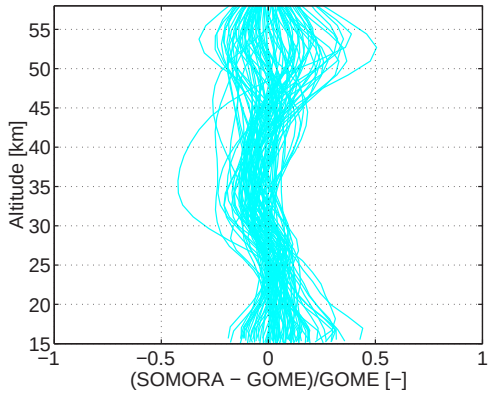

Figure 7: As Figure 6, but with profiles corrected for different a-priori information, optimized with respect to the comparison ensemble a-priori, and GOME profiles convoluted with SOMORA averaging kernels.

5. CONCLUSIONS

We proposed a simple method to regrid remote sensing observations of atmospheric constituents profiles. The method allows to homogenize the coordinates of different state vectors retrieved by different observing systems, without altering either retrieval procedure. By allowing an accurate control of the undertaken profile transformation process, it also improves the reliability of comparisons of homogenized state vectors. This method was applied to the comparison of remote sensing observations of the stratospheric ozone profile by the satellite borne Global Ozone Monitoring Experiment (GOME) and the ground-based millimeter-wave Stratospheric Ozone Monitoring Radiometer (SOMORA). A $\pm$ 20% (2σ-width) overall agreement was achieved between 84 coincident SOMORA and GOME measurements during 2000, after removal of all smoothing error contributions. The obtained comparison results were verified by means of a second series of microwave ozone profile retrievals, computed directly on the GOME retrieval grid. Validation of the proposed transformation method was achieved by showing that no systematic differences are observed in the results of intercomparisons performed in the SOMORA profile coordinates, or using the reprocessed microwave instrument dataset.

ACKNOWLEDGMENTS

The authors would like to thank Roeland van Oss for kindly providing the GOME level-2 ozone data and for his precious help in the description of the GOME measurements. Many thanks also to Clive D. Rodgers, for very useful comments on a previous paper version. This work was supported by MeteoSwiss and the Swiss National Science Foundation under grant 200020-100153.

REFERENCES

[1] Rodgers C. D. and B. J. Connor, Intercomparison of remote sounding instruments, *J. Geophys. Res.*, 108(D3), 4116, 2003, doi:10.1029/2002JD002299.

[2] Rodgers C. D., Characterization and error analysis of profiles retrieved from remote sounding measurements, *J. Geophys. Res.*, 95(D5), 5587–5595, 1990.

[3] Tsou J. J., B. J. Connor, A. Parrish, I. S. McDermid, and W. P. Chu, Ground-based microwave monitoring of middle atmosphere ozone: comparison to lidar and Stratospheric and Gas Experiment II satellite observations, *J. Geophys. Res.*, 100, 3005–3016, 1995.

[4] Connor B. J., A. Parrish, J.-J. Tsou, and M. P. McCormick, Error analysis for the ground-based microwave ozone measurements during STOIC, *J. Geophys. Res.*, 100(D5), 9283–9291, 1995.

[5] Rodgers C. D., *Inverse methods for atmospheric sounding*, volume 2 of *Series on atmospheric, oceanic, and planetary physics*, World Scientific, Singapore, 2000.

[6] Rodgers C. D., Retrieval of atmospheric temperature and composition from remote measurements of thermal radiation, *Rev. Geophys. Space Phys.*, 14(4), 609–624, 1976.

[7] R. H. Moore and M. Z. Nashed, Approximations to generalized inverses, MRC Tech. Summary Report 1294, University of Wisconsin, 1935.

[8] Penrose R., A generalized inverse for matrices, *Proc. Camb. Phil. Soc.*, 51, 406–413, 1955.

[9] Burrows J. P. et al., The Global Ozone Monitoring Experiment (GOME): mission concept and first scientific results, *J. Atmos. Sci.*, 56, 151–175, 1999.

[10] Calisesi Y., The Stratospheric Ozone Monitoring Radiometer SOMORA: NDSC application document, Research Report 2003-11, Institute of Applied Physics, University of Bern, Switzerland, 2003.

[11] Calisesi Y., The Stratospheric Ozone MOnitoring RAdiometer SOMORA: Data retrieval, Research Report 2000-3, Institute of Applied Physics, University of Bern, Switzerland, 2000.

[12] Fortuin J. P. F. and H. Kelder, An ozone climatology based on ozonesonde and satellite measurements, *J. Geophys. Res.*, 103, 31709–31734, 1998.